Dyes and Pigments 99 (2013) 480–488

Contents lists available at SciVerse ScienceDirect

Dyes and Pigments

journal homepage: www.elsevier.com/locate/dyepig

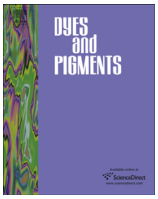

Synthesis, fluorescence, excited triplet state properties and singlet oxygen generation of *para*-(*tert*-butylphenoxy) substituted phthalocyanines containing group IV A central elements

Xian-Fu Zhang [a,b,*], Xiaona Shao [a], Hongyan Tian [a], Xiaojie Sun [a], Kaixue Han [a]

[a] *Chemistry Department, Hebei Normal University of Science and Technology, Qinhuangdao, Hebei Province 066004, China*
[b] *MPC Technology, Hamilton, ON L8S 3H4, Canada*

A R T I C L E I N F O

Article history:
Received 23 February 2013
Received in revised form
10 June 2013
Accepted 11 June 2013
Available online 18 June 2013

Keywords:
Phthalocyanine
Singlet oxygen
Triplet state
Fluorescence
Si–Ge–Sn–Pb
Photodynamic therapy (PDT)

A B S T R A C T

Phthalocyanines containing group IV A central elements and non-peripheral *para*-(*tert*-butyl)-phenoxy substituents, i.e. $M(OH)_2PC(\alpha\text{-}t\text{-butyl-phenoxy})_4$ (M is Si, Ge, Sn and Pb respectively), were synthesized. The effects of the central elements on the photosensitizing and photophysical properties (quantum yield of singlet oxygen formation, quantum yield and lifetime of lowest lying excited triplet- and singlet state) were investigated by laser flash photolysis, time correlated single photon counting, steady state fluorescence and absorption spectra. The incorporation of large atoms significantly enhances the efficiency of excited triplet state and singlet oxygen formation. The triplet quantum yield is increased 2.5 times to 0.75 for the lead tetrasubstituted phthalocyanine relative to that of 0.30 determined for the silyl analog, while the triplet lifetime is longer than 120 μs. Correspondingly, the quantum yield of singlet oxygen formation is 0.64 for the lead tetrasubstituted phthalocyanine and is 0.26 for the silyl compound. All of the PC complexes maintain reasonably good fluorescence characteristics with the shortest fluorescence lifetime measured being 3.14 ns, and the lowest fluorescence quantum yield of 0.18. These properties indicate that some of the PC complexes may be good candidates for singlet oxygen photosensitization.

1. Introduction

Photodynamic therapy (PDT) of tumors involving certain types of photosensitizers has been approved in clinic use for the treatment of several diseases [1–4]. A photosensitizer (PS) is a light-absorbing substance that generates reactive oxygen species (mainly singlet oxygen) and is not consumed in the reaction. Developing new PSs is currently an active field to address several needs in PDT [1–4], including (i) high light absorption within the optimal window (650–850 nm), (ii) a high quantum yield and long lifetime for the excited triplet state, (iii) a low tendency to form aggregates, (iv) amphiphilicity and (v) high selectivity for the target tissue.

Phthalocyanines (PCs) belong to a class of synthetic aromatic dyes which are structurally similar to the porphyrins [5–7]. Some PCs, especially Al, Zn and SiPC complexes, have been shown to be effective in PDT [1], the photophysical properties for these PCs have also been extensively studied [8–42]. Nonetheless, the photodynamic activity of many metal PC complexes (e.g. germanium PCs, tin PCs) has not been explored in depth, especially when compared to Al, Zn and Si PC complexes [1]. The incorporation of central metals with a high atomic number such as germanium, tin and lead, which enhance the intersystem crossing (ISC) from S_1 (the lowest lying excited singlet state) to T_1 (the lowest lying excited triplet state), is of current research interest, since this will increase the quantum yield of triplet state formation (Φ_T) and improve the quantum efficiency of singlet oxygen generation (Φ_Δ). This method to improve photosensitizing capability is actually one way to harness heavy atom effect (HAE) [43–45].

In this report a systematic study was made on group IV A (Si, Ge, Sn Pb) PC complexes (Fig. 1), which are all substituted at one α-position of each benzene moiety by a *para*-(*tert*-butyl)phenoxy. Various synthesis strategies were explored. All aspects of photophysics related to photosensitizing properties of the complexes were covered. For the β-substituted Ge and Sn PC complexes, Maree and Nyokong reported the synthesis and photosensitizing properties [46].

---

* Corresponding author. Chemistry Department, Hebei Normal University of Science and Technology, Qinhuangdao, Hebei Province 066004, China. Tel./fax: +86 0335 8387040.
E-mail addresses: zhangxianfu@tsinghua.org.cn, zhangxf111@hotmail.com (X.-F. Zhang).

0143-7208/$ – see front matter © 2013 Elsevier Ltd. All rights reserved.
http://dx.doi.org/10.1016/j.dyepig.2013.06.010

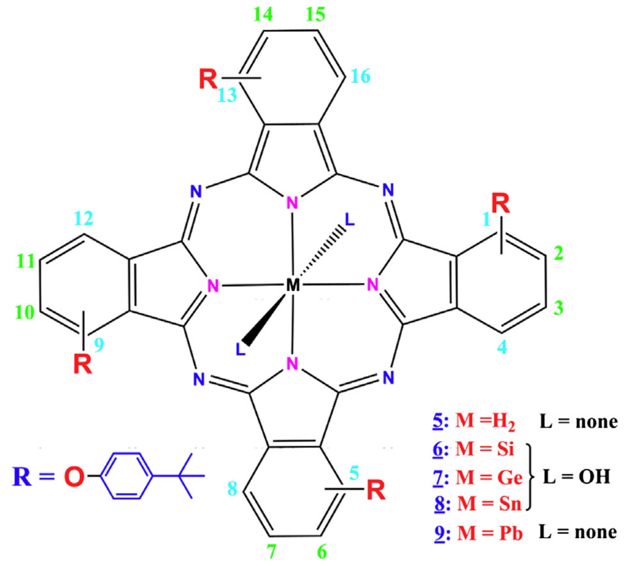

Fig. 1. Chemical structure of ML_2PCR_4 complexes **5** to **9**, R is located at 1, 5(8), 9(12), and 13(16), respectively.

2. Experimental

2.1. Reagents and apparatus

All reagents for synthesis were analytical grade and used as received. Ethanol and dimethylformide (DMF) were dried and redistilled before use. UV–visible spectra were recorded on a StellarNet BLACK Comet C-SR diode array miniature spectrophotometer connected to deuterium and halogen lamp by Optical fiber using 1 cm matched quartz cuvettes. A Shimadzu FTIR-8900 spectrometer was used to record IR spectra at room temperature. MS spectra were recorded either on a Bruker APEX II or Autoflex III Maldi-TOF spectrometer. The measurement of ^1H NMR spectra was carried out at room temperature on a Bruker DMX 400 MHz NMR spectrometer.

2.2. Synthesis

2.2.1. Synthesis of 3-(4-tert-butylphenoxy)phthalonitrile (3)

3-Nitrophthalonitrile (1.73 g, 0.01 mol) and 4-*tert*-butylphenol (1.50 g, 0.01 mol) were dissolved in DMSO (30 mL), LiOH (0.42 g, 0.01 mol) was then added. The resulted mixture was then stirred at 50 °C for 24 h under N_2 atmosphere. The product solution was cooled and then poured into NaCl solution (10% aqueous, 100 mL), the precipitated solid was filtered, washed with water and dried under vacuum. White needles were obtained after recrystallization in toluene. Yield: 51%. m.p. 116–118 °C. IR (KBr), ν(cm^{-1}): 3083, 3014, 2232 (C≡N), 1695, 1632, 1563, 1506, 1485, 1465, 1429, 1386, 1351, 1275 (C–O–C), 1258, 1222, 1165, 1142, 1015, 938, 917. ^1H NMR (400 MHZ, $CDCl_3$, ppm): δ 1.353 (s, 9H, *t*-butyl), 6.992 (d, 2H, J = 7 Hz, Ar–H), 7.245 (d, 1H, J = 6 Hz, Ar–H), 7.510 (d, 2H, J = 7 Hz, Ar–H), 7.799 (m, 2H, Ar–H), 7.835 (m, 1H, Ar–H). MS, *m/z*: 298.95 $[M + Na]^+$.

2.2.2. Synthesis of tetra(α–4-tert-butylphenoxy) phthalocyanine, H_2PcR_4 (5)

3-(4-*tert*-Butylphenoxy)phthalonitrile (0.276 g, 1 mmol) and dried N,N-dimethylamino-ethanol (5 mL) were mixed and stirred at 150 °C for 4 h under argon atmosphere in the presence of two drops of DBU as catalyst. After cooling down, water (50 mL) was added and the green precipitate was filtered and washed with water. The dried crude product was dissolved in dichloromethane and purified by column chromatography (silica gel) using dichloromethane as the mobile phase. Yield: 39%. UV–vis (EtOH): λ_{max} nm 334, 691, 717. IR [(KBr) ν_{max}/cm^{-1}]: 750, 941, 1256, 1412, 1589, 1697 (PC ring); 1335, 1412, 2953, 2961 (CH_3); 1026, 1175 (Ar–O–C). ^1H NMR ($CDCl_3$): δ, ppm 7.49–7.89 (12H, m, Pc–H), 7.01–7.47 (16H, m, phenyl–H), 1.21–1.65 (36H, m, CH_3). MALDI-TOF-MS *m/z*: Calculated 1107.4; found 1107.6 $[M + 1]^+$. Calcd. for $C_{72}H_{66}N_8O_4$ C, 78.09: H, 6.01; N, 10.12. Found: C 77.58, H, 6.21; N, 10.27.

2.2.3. Synthesis of tetra(α–4-tert-butylphenoxy) silicon phthalocyanine, $Si(OH)_2PcR_4$ (6)

Compound 3-(4-*tert*-butylphenoxy)phthalonitrile was converted to 3-(4-*tert*-butylphenoxy)1,3-diiminoisoindoline in the first step. To methanol (40 mL) containing CH_3ONa (0.070 g, 1.4 mmol), 3-(4-*tert*-butylphenoxy)phthalonitrile (2.76 g, 10 mmol) was added. Ammonia was then bubbled through the solution with stirring for 1 h at room temperature. The temperature was then raised to 70 °C and the reaction was maintained for 9 more hrs with stirring and N_2 bubbling. After cooling down, methanol was removed by distillation. The solid was then washed with water, filtered, and dried under vacuum.

3-(4-*tert*-Butylphenoxy)1,3-diiminoisoindoline (0.55 g, 1.86 mmol) and $SiCl_4$ (0.30 mL, 2.63 mmol) were added into freshly distilled quinoline (3 mL) and stirred at 200 °C under argon for 1 h. Acetone (10 mL) was added, the resulted mixture was filtered and washed with acetone. The filtrate and the solvent were evaporated under vacuum. The product was purified by column chromatography (silica gel) by using CH_2Cl_2 as eluent. Yield: 27%. UV–vis (EtOH): λ_{max} nm 346, 699. IR [(KBr) ν_{max}/cm^{-1}]: 617, 748, 982, 1252, 1479, 1589 (PC ring); 1015 (Si–O); 1335, 2868, 2903, 2961 (CH_3); 1070, 1245 (Ar–O–C). ^1H NMR ($CDCl_3$): δ, ppm 7.57–7.95 (12H, m, Pc–H), 7.03–7.62 (16H, m, phenyl–H), 1.21–1.69 (36H, m, CH_3). MALDI-TOF-MS *m/z*: Calculated 1166.5; found 1149.5 $[M - OH]^-$. Calcd. for $C_{72}H_{66}N_8O_6Si$ C, 74.07; H, 5.70; N, 9.60. Found: C, 73.66; H, 5.51; N, 9.39.

2.2.4. Synthesis of tetra(α–4-tert-butylphenoxy) germanium phthalocyanine, $Ge(OH)_2PcR_4$ (7)

Tetra(α–4-*tert*-butylphenoxy) phthalocyanine (0.31 g, 0.28 mmol) and freshly distilled quinoline (5 mL) were added into 25 mL three-necked flask. After bubbling argon for 10 min, $GeCl_4$ (0.5 mL, 4.4 mmol) was added quickly. The solution was stirred for 2 h at 240 °C. After cooling down, acetone (10 mL) was added, the resulting mixture was filtered and washed with acetone. The filtrate and the solvent were evaporated under vacuum. The product was purified by column chromatography (silica gel) by using CH_2Cl_2 as eluent. Yield: 33%. UV–vis (EtOH): λ_{max} nm 342, 714. IR [(KBr) ν_{max}/cm^{-1}]: 640, 743, 972, 1259, 1483, 1589 (PC ring); 1015 (Ge–O); 1340, 2866, 2963 (CH_3); 1080, 1213 (Ar–O–C). ^1H NMR ($CDCl_3$): δ, ppm 7.60–8.01 (12H, m, Pc–H), 7.06–7.59 (16H, m, phenyl–H), 1.17–1.75 (36H, m, CH_3). MALDI-TOF-MS *m/z*: Calculated 1212.4; found 1195.5 $[M\text{-}OH]^-$. Calcd. for $C_{72}H_{66}GeN_8O_6$ C, 71.35; H, 5.49; N, 9.25. Found: C, 70.79; H, 5.09; N, 9.47.

2.2.5. Synthesis of tetra(α–4-tert-butylphenoxy) tin phthalocyanine, $Sn(OH)_2PcR_4$ (8)

3-(4-*tert*-Butylphenoxy)phthalonitrile (0.276 g, 1 mmol) and dried *N,N*-dimethylaminoethanol (5 mL) were mixed and stirred at 150 °C for 4 h under argon atmosphere in the presence of two drops of DBU as catalyst. $SnCl_2$ (0.19 g, 1 mmol) was then added at 170 °C, the reaction was maintained for 1 h. After cooling, water (50 mL) was added and the green precipitate was collected by filtration and washed with water. The dried crude product was dissolved in dichloromethane and purified by column chromatography (silica gel) using dichloromethane as the mobile phase. Yield: 43%. UV–vis (EtOH): λ_{max} nm 331, 624, 691. IR [(KBr) ν_{max}/cm^{-1}]: 608, 827, 972, 1259, 1477, 1593, 1651 (PC ring); 1047 (Sn–O); 1339, 1364, 1396, 2868, 2963 (CH_3); 1090, 1211 (Ar–O–C). ^{1}H NMR ($CDCl_3$): δ, ppm 9.20–9.42 (4H, m, Pc-H), 8.91–9.12 (4H, m, Pc-H), 8.00–8.23 (4H, m, Pc-H), 7.55–7.80 (16H, m, phenyl-H), 1.30–1.62 (36H, m, *t*-butyl). MALDI-TOF-MS *m*/*z*: Calculated 1258.4; found 1241.5 $[M - OH]^-$. Calcd. for $C_{72}H_{66}N_8O_6Sn$ C, 68.74; H, 5.29; N, 8.91. Found: C, 68.29; H, 5.58; N, 8.46.

2.2.6. Synthesis of tetra(α–4-tert-butylphenoxy) lead phthalocyanine, PbPcR$_4$ (**9**)

To a DMF solution of tetra(α–4-*tert*-butylphenoxy) phthalocyanine (59 mg, 0.05 mmol), lead diacetate (11.9 mg, 0.05 mmol) was added. The resulted solution was stirred under argon atmosphere at 200 °C for 1.5 h. After cooling, water (50 mL) was added and the green precipitate was collected by filtration and washed with water. The dried crude product was dissolved in dichloromethane and purified by column chromatography (silica gel) using dichloromethane as the mobile phase. Yield: 57%. UV–vis (EtOH): λ_{max}/nm 331, 624, 691. IR [(KBr) ν_{max}/cm^{-1}]: 644, 748, 974, 1250, 1477, 1508, 1597 (PC ring); 1015 (Pb–O); 1331, 1364, 2866, 2959 (CH_3); 1065, 1213 (Ar–O–C). ^{1}H NMR (DMSO): δ, ppm 8.39–9.04 (12H, m, Pc–H), 7.71–8.01 (16H, m, phenyl–H), 1.29–1.34 (36H, m, CH_3). MALDI-TOF-MS *m*/*z*: Calculated 1312.5; found 1313.3 $[M + H]^+$. Calcd. for $C_{72}H_{64}N_8O_4Pb$ C, 65.89; H, 4.91; N, 8.54. Found: C, 66.49; H, 4.52; N, 8.37.

2.3. Photophysical measurements

2.3.1. Fluorescence

Fluorescence spectra and lifetimes were acquired on a FLS 920 of Edinburgh Instruments using 1 cm quartz cuvettes. All fluorescence spectra were corrected for the sensitivity of the photo-multiplier tube. The absorption, fluorescence and excited triplet state properties were investigated at room temperature (22 °C). All ethanol solutions were air saturated for absorption, fluorescence spectra and fluorescence quantum yield (Φ_f) measurements.

Φ_f was computed by Eq. (1)

$$\Phi_f = \Phi_f^0 \cdot \frac{\mathbf{F}_s}{\mathbf{F}_0} \cdot \frac{\mathbf{A}_0}{\mathbf{A}_s} \frac{{n_s}^2}{{n_0}^2}, \tag{1}$$

in which **A** is the absorbance at excitation wavelength, **F** is the integrated fluorescence intensity, *n* is the refractive index of the solvent, the subscript 0 stands for a reference compound and s represents samples. ZnPc was used as the reference ($\Phi_f^0 = 0.18$) in DMSO [47]. The excitation wavelength is 610 nm, which is corresponding to the vibronic band of S_0 to S_1 transitions. The absorbance of a sample and the reference solutions was adjusted so that they both have roughly the same absorbance (A_i is about 0.050) at the excitation wavelength.

Time-correlated single photon counting method was used to measure fluorescence lifetime (τ_f) with excitation at 672 nm by a diode laser (70 ps FWHM), the emission was monitored at the wavelength of a band maximum. τ_f was obtained by a convolution procedure that fits the summation of IRF and $I(0)e(-t/\tau_f) + B$ to the measure $I(t)$, in which IRF is the measured instrument response, $I(t)$ is the fluorescence intensity at time t after laser excitation, B is a constant (fluorescence background). The software is a product of the instrument supplier.

2.3.2. Laser flash photolysis

An Edinburgh LP920 laser flash photolysis system was used to obtain transient absorption spectra in DMF. The concentrations of the target compounds were typically 15 μM providing $A_{355} = 0.30$ in 10 mm cuvettes. The solutions were either air-saturated or deoxygenated by bubbling with argon for 20 min in a capped quartz cuvettes. The optical path length was 1 cm. The excitation source was A Nd:YAG laser (Brio, 355 nm and 4 ns FWHM). The analyzing light was from a pulsed xenon lamp, perpendicular to the excitation laser. The signal was recorded on a R928B detector and displayed by a Tektronix TDS 3012B oscilloscope. The laser energy incident at the sample was attenuated to ca. 10 mJ per pulse. Time profiles at a series of wavelengths were recorded with the aid of a computer controlled kinetic absorption spectrometer, from which point by-point spectra were sliced and assembled by the L900 software provided by the instrument supplier.

The triplet quantum yield (Φ_T) was computed by Eq. (2) by using ZnPc ($\Phi_T = 0.65$ in 1-propanol) as a reference [48],

$$\Phi_T = \Phi_T^{ZnPc} \cdot \frac{\Delta\varepsilon_T^{ZnPc}}{\Delta A_T^{ZnPc}} \cdot \frac{\Delta A_T}{\Delta\varepsilon_T}, \tag{2}$$

in which ΔA_T is the absorbance of the triplet–triplet absorption spectrum at the selected wavelength, and $\Delta\varepsilon_T$ is the triplet state molar absorption coefficient. $\Delta\varepsilon_T$ of the samples were obtained by using the singlet depletion method according to Eq. (3) [48].

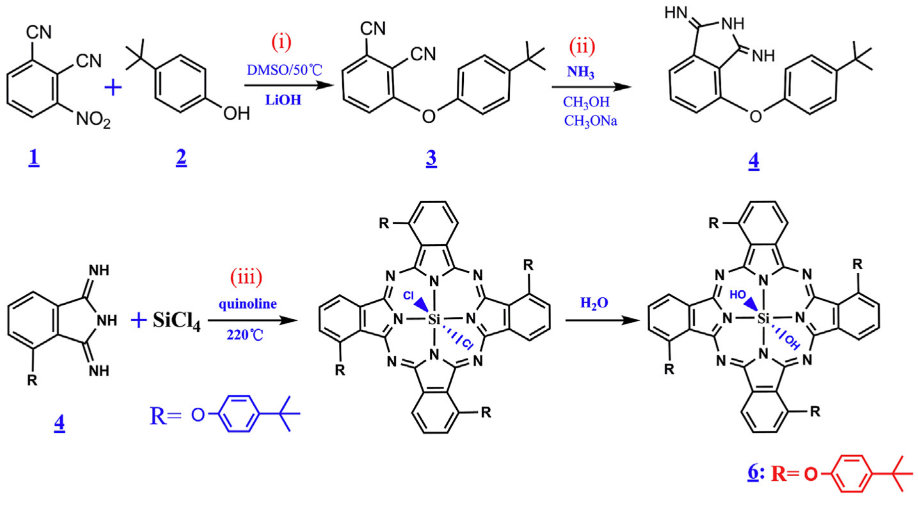

Fig. 2. The synthetic route for SiPcR$_4$.

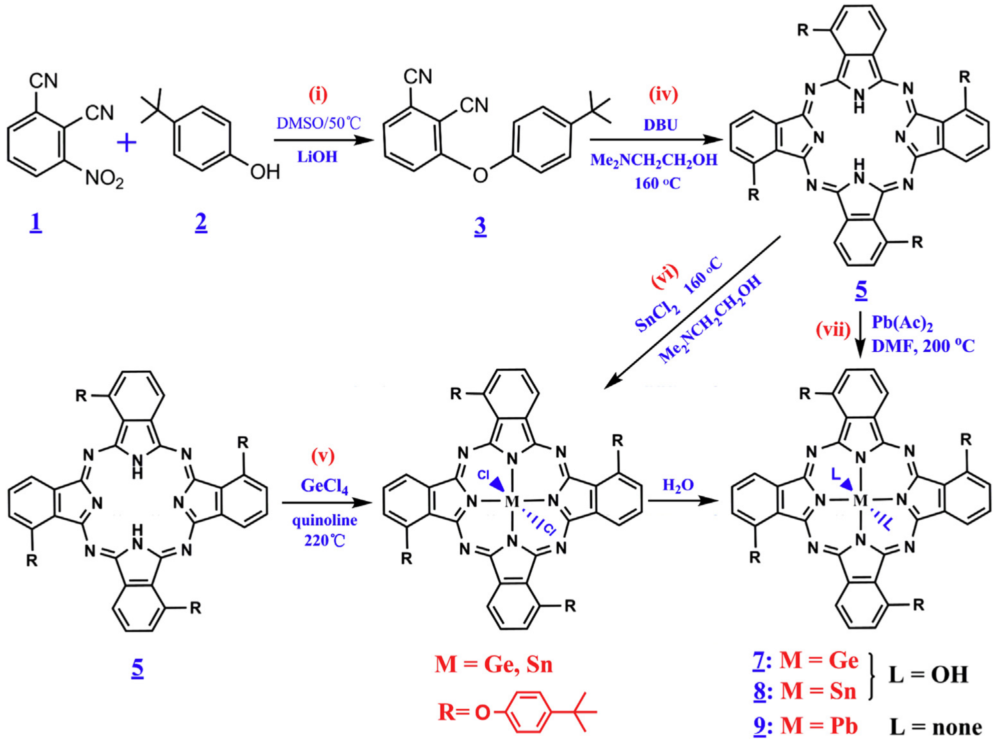

Fig. 3. The synthetic route for GePCR$_4$, SnPcR$_4$ and PbPcR$_4$.

$$\Delta\varepsilon_T = \varepsilon_S \frac{\Delta A_T}{\Delta A_S} \qquad (3)$$

ε_S is the molar absorption coefficient at the UV–vis absorption band maximum for the ground-state. ΔA_S and ΔA_T in Eq. (3) are the absorbance change at the minimum of the bleaching band and the maximum of the positive band, respectively. Both ΔA_S and ΔA_T were obtained from the triplet transient difference absorption spectra.

2.3.3. Singlet oxygen generation

Singlet oxygen quantum yields (Φ_Δ) were determined by the chemical trapping method, since one molecule of singlet oxygen can react with one molecule of diphenylisobenzofuran (DPBF) which causes DPBF bleaching [49]. Typically, a 3 mL portion of the respective 5 μM PS solution that contained 30 μM DPBF was irradiated by a LED lamp (660 nm) from StellarNet corp. in air saturated DMF. Φ_Δ value was calculated by Eq. (4) using ZnPc as the reference (Eq. (4)):

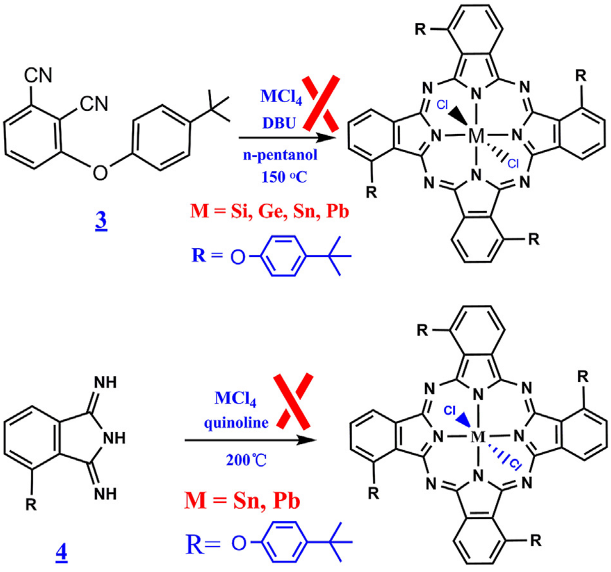

Fig. 4. The synthetic routes that did not lead to the desired product.

$$\Phi_\Delta = \Phi_\Delta^{ref} \frac{k}{k^{ref}} \frac{I_a^{ref}}{I_a}, \qquad (4)$$

where Φ_Δ^{ref} is the singlet oxygen quantum yield for the standard (0.56 for ZnPc in DMF) [50], k and k^{ref} is the DPBF photo-bleaching rate constant for the sample and ZnPc, respectively; I_a and I_a^{ref} is the rate of light absorption at the irradiation wavelength of 660 nm by the sample and standard, respectively. Their ratio can be obtained by Eq. (5).

$$\frac{I_a^{ref}}{I_a} = \frac{1-10^{-A_{670}^{ref}}}{1-10^{-A_{670}}}, \qquad (5)$$

DPBF degradation was monitored by UV–vis absorption spectrum. The error in the determination of Φ_Δ was ~10% (determined from several Φ_Δ values).

3. Results and discussion

3.1. Synthesis

The synthetic routes to the desired products are shown in Figs. 2 and 3. K_2CO_3, a base that is often effective in the reaction of a phenol with nitro substituted phthalonitrile at room temperature, did not work well in reaction (i) that generates compound **3**. Instead, a strong base LiOH and a higher temperature were needed to effect reaction (i). Initial attempts to prepare the PCs **6**, **7**, **8**, **9** by the very common procedure (Fig. 4) by using the condensation of compound **3** with $PbCl_4$ (or $Pb(CH_3COO)_2$) or $SnCl_4$ were not successful, although the common method (Fig. 4 top) worked well for $MPCR_4$ (M = Zn, Cu, InCl, GaCl, TiO) [51–54].

Table 1
The photophysical properties of compounds ML_2PCR_4 in ethanol.[a]

	λ_{abs}, nm	λ_{ex}, nm	λ_{em}, nm	Φ_f	τ_f, ns	Φ_T	τ_T, μs	λ_{T-T},nm	Φ_Δ	k_f, 10^9 s^{-1}
$Si(OH)_2PcR_4$	699	698	718	0.66	5.29	0.30	267	593	0.26	0.13
$Ge(OH)_2PcR_4$	711	714	725	0.52	4.23	0.34	129	565	0.30	0.12
$Sn(OH)_2PcR_4$	691	690	706	0.45	3.14	0.43	125	553	0.36	0.14
$PbPcR_4$	691	691	707	0.18	3.21	0.75	121	578	0.64	0.055

[a] λ_{abs}: absorption maximum. λ_{ex}: excitation maximum. λ_{em}: emission maximum. Φ_f: fluorescence quantum yield. τ_f: fluorescence lifetime. χ^2: chi square values for τ_f fitting is within 1.00–1.03. τ_T: triplet lifetime. Φ_T: quantum yield for triplet state. λ_{T-T}: T_1–T_n absorption maximum. Φ_Δ: quantum yield for singlet oxygen. k_f: the rate constant of emission process, calculated by $k_f = \Phi_f/\tau_f$.

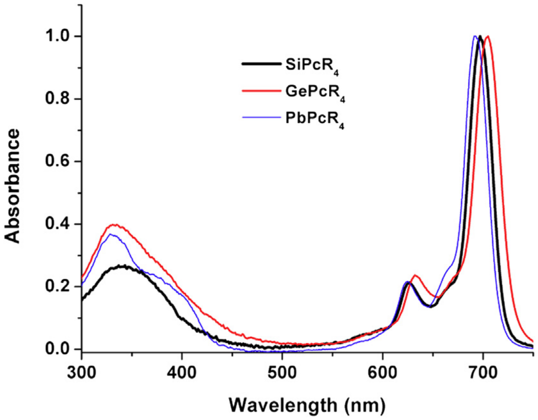

Fig. 5. Normalized UV–vis absorption spectra of $MPcR_4$ in ethanol.

Two different pathways are required to obtain the four phthalocyanines in this study. For $Si(OH)_2PcR_4$, reaction (iii) in Fig. 2 was employed in which compound **4** was the starting material. This procedure, however, did not work for $Sn(OH)_2PcR_4$ and $PbPcR_4$. Reaction (v) in Fig. 3 proved to be successful in which Ge was inserted into the isolated metal-free phthalocyanine **5** in quinoline. Reaction (vi) and (vii) are necessary to prepare $Sn(OH)_2PcR_4$ and $PbPcR_4$, but **5** was not isolated during the one-pot two-step reaction, in which the first step was to allow **5** to form. The reaction did not lead to **8** (or **9**) when **3** and $SnCl_2$ (or $PbAc_2$) were heated under reflux in n-pentanol in the presence of DBU.

3.2. Photophysics

Table 1 summarizes the photophysical properties of compounds **6**, **7**, **8**, **9**. Both the fluorescence and triplet excited state properties are affected significantly by the change of the central element. The increase of atom size remarkably enhances the efficiency of triplet state and singlet oxygen formation whilst good fluorescence characteristics were retained. The details of these properties are described in the following section.

3.2.1. Ground state UV–vis absorption spectra

The UV–vis absorption spectra of the phthalocyanines in ethanol or DMF all showed similar spectral behavior, and the spectra shown in Fig. 5 are typical. It can be seen that the Q band of $Si(OH)_2PcR_4$ shows a vibronic shoulder with an intense narrow peak at 699 nm, while the B band is located at 331 nm. $Ge(OH)_2PcR_4$ Q band showed a red-shifted maximum (711 nm) relative to that of $Si(OH)_2PcR_4$. $Sn(OH)_2PcR_4$, $PbPcR_4$, however, exhibited blue-shifted Q band maxima (both are 691 nm) relative to that of $SiPcR_4$. The absorption maxima (λ_{abs}) are included in Table 1.

The blue shift is a reflection of the planarity of the π-system. With the increase of the atomic size from Si to Pb, Pb and Sn cannot be inserted into the cavity of PC but are located outside PC π-ring. The mutual interaction leads to the deviation of PbPC ring from planarity to a shuttlecock shaped structure [55–57].

The Beer–Lambert law plots for all of the compounds in ethanol showed good linearity in the range of concentrations investigated (0.50–20 μM), indicating no aggregation in the ground state.

3.2.2. Fluorescence properties

The fluorescence emission spectra of ML_2PcR_4 are compared in Fig. 6. Their spectral shape are all similar and typical of that for PCs, although the maximal wavelengths of the emission peaks are influenced by the central elements. Table 1 includes the excitation and emission maxima (λ_{ex} and λ_{em}). The effect of the central elements on λ_{ex} or λ_{em} is the same as their influence on λ_{abs} (Table 1).

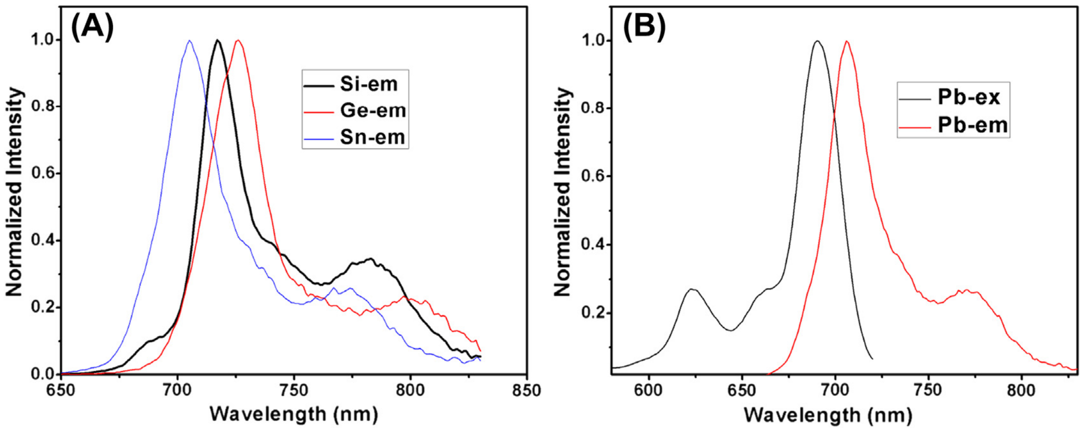

Fig. 6. (**A**) The normalized fluorescence emission spectra of $MPcR_4$ (M = Si, Ge, Sn) in EtOH with excitation at 610 nm (absorbance 0.050). (**B**) The normalized excitation (emission at 730 nm) and emission spectra of $PbPcR_4$ in EtOH (with excitation at 610 nm).

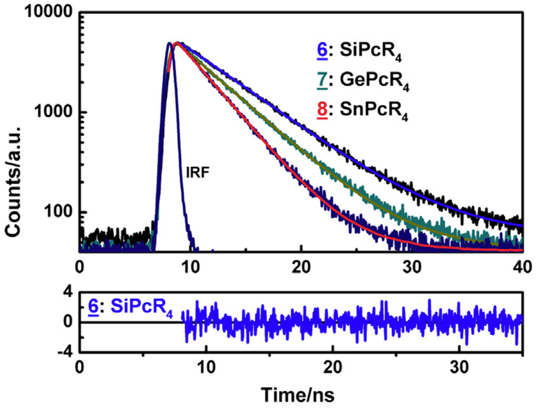

Fig. 7. Fluorescence decay of MPCR$_4$ (M = Si, Ge, Sn) in EtOH with excitation at 672 nm diode laser (70 ps), the emission was monitored at emission maximum, the concentration of dyes is ca. 2.0 μM. **Bottom**: fitting residues for SiPCR$_4$.

The symmetry between the excitation and emission spectra holds for all ML$_2$PCR$_4$ compounds. The stokes shift were about 17(±3) nm, the small values indicate only a slight change of the molecular geometry upon photoexcitation.

The fluorescence decays in Fig. 7 are satisfactorily described by monoexponential functions. In all cases, the weighted residuals (Fig. 7 bottom) are small, and the reduced chi-squared values (χ^2 in Table 1) are 1.02 ± 0.02, indicating a good agreement of the monoexponential fits. The decay lifetimes (τ_f) are given in Table 1.

Φ_f is monotonically lowered with the increase of atomic size (Table 1). So is the case for τ_f. This lowering of Φ_f and τ_f is generally due to the enhancement of the spin-orbit coupling between *d*-orbitals of the metal ion and PC π-ring electrons. The angular movement of the electron through the magnetic field created by the atomic nucleus can impart an electromagnetic force on the electron causing it to change its spin. This can only occur if the electron is alone in an orbital and thus free from the influences of another electron (the case in S$_1$ state). The Hamiltonian for spin-orbit interaction (H_{s-o}) is strongly proportional to the nuclear charge as shown in Eq. (6), which is intractably proportional to the size of the atom [58].

$$H_{s-o} = \frac{z^4 e^2}{8\pi\varepsilon_0 m_e^2 c^2}\boldsymbol{L}\cdot\boldsymbol{S}, \tag{6}$$

In which e is the elementary charge of an electron, ε_0 is the permittivity of the vacuum, m_e is the mass of an electron, c is the speed of light, and z is the atomic number of the acting nucleus. The vector portion is the dot product of the electron's angular momentum, $\boldsymbol{L}$, and spin, $\boldsymbol{S}$. The magnitude of spin-orbit coupling is thus greatly affected by the size of the nucleus.

The stronger spin-orbit coupling results in the faster ISC from S$_1$ to T$_1$, i.e. a larger k_{isc} arises, which leads to a smaller Φ_f and τ_f, since $\tau_f = (k_f + k_{ic} + k_{isc})^{-1}$, and $\Phi_f = k_f/(k_f + k_{ic} + k_{isc})$. k_f can be obtained by $k_f = \Phi_f/\tau_f$, the values are also included in Table 1. k$_f$ values for the three ML$_2$PCR$_4$ (M = Si, Ge, Sn) are about the same, ca. 0.13×10^9 s^{-1}, but reduced remarkably to 0.55×10^8 s^{-1} for PbPCR$_4$. The decrease of k_f in PbPCR$_4$ is due to the significant bending of the PbPC π-system, so that a strain force exists and favors the internal conversion by heat release.

3.3. Triplet excited state properties

The transient absorption spectra for the PC complexes are displayed in Fig. 8. Laser flash photolysis (LFP) was carried out with laser excitation (4 ns) pulse at 355 nm. The samples for the spectra were dissolved in DMF and purged with argon for 20 min before the measurement. The transient spectra show common features: **1**) the

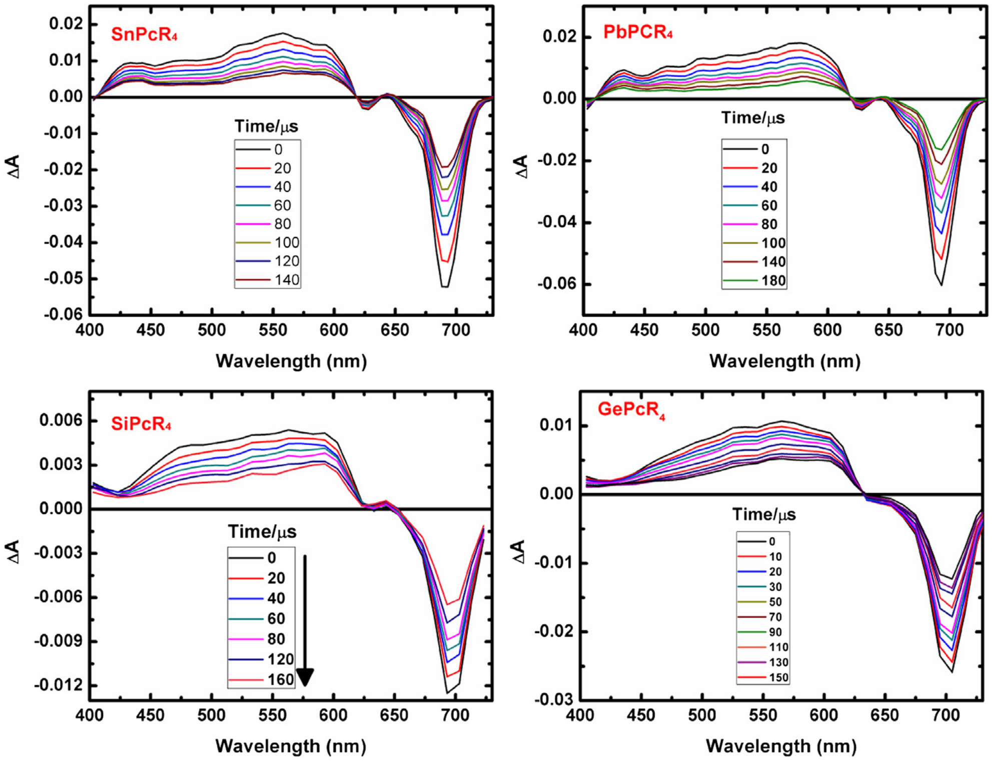

Fig. 8. The transient absorption spectra in argon saturated DMF with laser excitation (4 ns) at 355 nm (absorbance was adjusted to ~0.3).

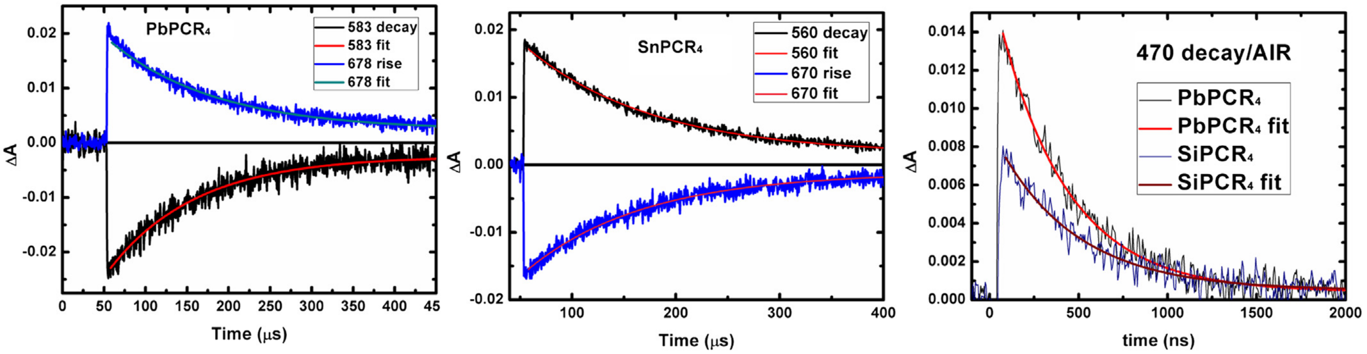

Fig. 9. Triplet decays and ground state recovery of $MPCR_4$ in argon saturated DMF (left and middle). Triplet decays in air saturated DMF with laser excitation (4 ns) at 355 nm (right).

negative absorption in the Q-band region showed peaks matching the corresponding ground state absorption; **2**) the broad shape of the positive absorption is similar to the T_1–T_n transient spectra found previously for other similar PCs [33,59–61]; **3**) the positive bands are separated from the ground state bleaching with well defined isosbestic points; **4**) the decrease of the positive band is accompanied by the increase of the negative band; **5**) the bleaching recovery kinetics is synchronous with the absorption decay kinetics (shown in Fig. 9). The concurrent behavior indicates that as the positive absorbing transient decays, the ground state is repopulated. In summary, the positive absorptions are due to T_1–T_n absorption decay while the negative bands are attributed to the recovery of S_0–S_1 absorptions; the spectral changes with time reflect a two state transformation: $T_1 \rightarrow S_0$.

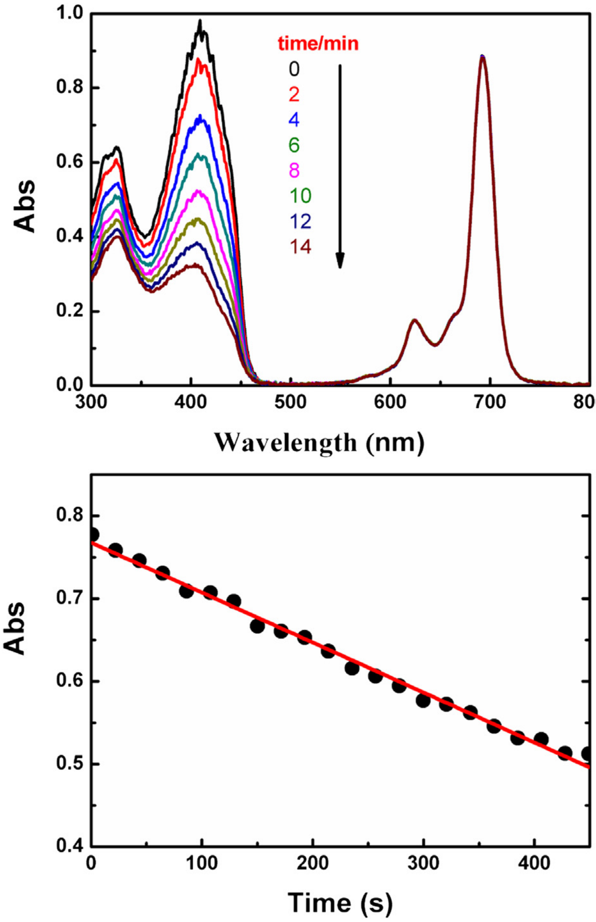

Fig. 10. Top: The variation of the absorption spectra in $Sn(OH)_2PcR_4$ (6 μM) photosensitized system containing 32 μM DPBF in DMF, with irradiation at 660 nm. Bottom: The plot of DPBF absorbance at 410 nm against time, and the linear fitting.

The T_1–T_n absorption maximum (λ_{T-T} in Table 1) is a function of the central elements. λ_{T-T} decreases with the atomic size, but $PbPCR_4$ showed slightly different behavior (Table 1).

Typical transient decay curves are given in Fig. 5. The synchronous ground state recovery is also shown. These curves can all be fitted by the monoexponential function. The triplet lifetimes are collected in Table 1. The τ_T values are all larger than 120 μs, the PC complex with a heavy central metal exhibits shorter τ_T values than that of $Si(OH)_2PCR_4$. The lifetimes are comparable to those of other PCs [48], and are sufficiently long for photosensitizing the production of singlet oxygen.

In air saturated DMF the triplet species decayed at a much faster rate (Fig. 9 right), the τ_T values are 0.45, 0.54, 0.38 and 0.39 μs for ML_2PCR_4 (M = Si, Ge, Sn, Pb), respectively. This is due to a very efficient molecular oxygen quenching. The rate constants by oxygen quenching (k_{et}) range from $0.92 \times 10^9\ M^{-1}\ s^{-1}$ to $1.31 \times 10^9\ M^{-1}\ s^{-1}$. The values are close to one-ninth of the diffusion rate of O_2 in the solvent.

This effective oxygen quenching also indicates that the positive absorptions are due to T_1–T_n triplet absorptions. The k_{et} values obtained above are comparable to the rate constants obtained for O_2 quenching of the triplet excited states of a variety of porphyrins and phthalocyanines [62].

Φ_T for each of the four compounds in DMF is given in Table 1. In contrast to Φ_f change, Φ_T becomes larger with increasing the atomic size, as shown in Table 1. The incorporation of large atoms significantly enhances the efficiency of triplet state formation. Φ_T is increased 2.5 times to 0.75 for $PbPCR_4$ from 0.30 for $Si(OH)_2PCR_4$, indicating an effective heavy atom effect. The summation of Φ_T and Φ_f in all cases is less than 1, suggesting the presence of internal conversion.

3.4. Singlet oxygen formation by DPBF chemical trapping

The quantum yields for singlet oxygen formation (Φ_Δ) were measured in air saturated DMF by using the chemical trapping method with irradiation at 660 nm. Photosensitized DPBF degradation was monitored by UV–vis spectroscopy. Fig. 10 displays the variation of DPBF absorbance upon irradiation, for which the pseudo zero-order kinetics could be applied (Fig. 10).

Φ_Δ is also collected in Table 1. The coordination of large atoms remarkably enhances the efficiency of singlet oxygen formation.

The value of Φ_Δ for each PC is close to its Φ_T, suggesting a good efficiency of energy transfer, considering the two competing processes:

$$T_1(PS) + {}^3O_2 \xrightarrow{k_{et}} S_0(PS) + {}^1O_2, \quad T_1 \text{ energy transfer to form singlet oxygen}$$

$$T_1(PS) \xrightarrow{k_d} S_0(PS), \quad T_1 \text{ natural decay}$$

since $k_{et}[O_2]$ values are 1.84–2.56 × 10^6 s^{-1}, which is 300 times larger than that of the competing decay rate of T_1 itself ($k_d = 1/\tau_T$), k_d values are 0.38–0.82 × 10^4 s^{-1}).

4. Conclusions

We have synthesized ML_2PCR_4 compounds in which M is Si, Ge, Sn, and Pb respectively, which includes all possible group IV elements in the periodic table. The preparation is not trivial since the common procedures reported in literature by using the condensation of compound **3** failed. The ML_2PCR_4 compounds harness the heavy atom effect to enhance triplet and singlet oxygen formation.

The photophysical and photochemical processes related to PDT were revealed by comparing the steady state and transient spectra of S_0, S_1, and T_1 of these compounds. The insertion of large atoms into PC complexes significantly enhances the efficiency of triplet state and singlet oxygen formation. The triplet quantum yield is increased 2.5 times to 0.75 for $PbPCR_4$ from 0.30 for $Si(OH)_2PCR_4$, while the triplet lifetime is longer than 120 μs. Correspondingly, the quantum yield of singlet oxygen formation is promoted to 0.64 for $PbPCR_4$ from 0.26 for $Si(OH)_2PCR_4$. In the mean time, these PC complexes still maintain reasonably good fluorescence characteristics. These properties indicate that some of the PC complexes are good candidates for singlet oxygen photosensitizers but the toxicity of lead compounds to the human body must be noted.

Acknowledgments

This work has been supported partially by Hebei Provincial Science Foundation (Contract B2010001518) and HBUST (Contract CXTD2012-05).

References

[1] Kudinova NV, Berezov TT. Photodynamic therapy of cancer: search for ideal photosensitizer. Biochem (Moscow) Suppl Ser B Biomed Chem 2010;4:95–103.

[2] Moreira LM, dos Santos FV, Lyon JP, Maftoum-Costa M, Pacheco-Soares C, da Silva NS. Photodynamic therapy: porphyrins and phthalocyanines as photosensitizers. Aust J Chem 2008;61:741–54.

[3] Josefsen LB, Boyle RW. Photodynamic therapy: novel third-generation photosensitizers one step closer? Br J Pharmacol 2008;154:1–3.

[4] O'Connor AE, Gallagher WM, Byrne AT. Porphyrin and nonporphyrin photosensitizers in oncology: preclinical and clinical advances in photodynamic therapy. Photochem Photobiol 2009;85:1053–74.

[5] Ishii K. Functional singlet oxygen generators based on phthalocyanines. Coord Chem Rev 2012;256:1556–68.

[6] McKeown NB. Phthalocyanine materials: synthesis, structure and function. Cambridge: Cambridge University Press; 1998.

[7] Bonnett R. Photosensitizers of the porphyrin and phthalocyanine series for photodynamic therapy. Chem Soc Rev 1995;24:19–33.

[8] Nyokong T. Effects of substituents on the photochemical and photophysical properties of main group metal phthalocyanines. Coord Chem Rev 2007;251:1707–22.

[9] Masilela N, Kleyi P, Tshentu Z, Priniotakis G, Westbroek P, Nyokong T. Photodynamic inactivation of *Staphylococcus aureus* using low symmetrically substituted phthalocyanines supported on a polystyrene polymer fiber. Dyes Pigment 2013;96:500–8.

[10] Zheng BY, Lin T, Yang HH, Huang JD. Photodynamic inactivation of *Candida albicans* sensitized by a series of novel axially di-substituted silicon (IV) phthalocyanines. Dyes Pigment 2013;96:547–53.

[11] Hota R, Baek K, Yun G, Kim Y, Jung H, Park KM, et al. Self-assembled, covalently linked, hollow phthalocyanine nanospheres. Chem Sci 2013;4:339–44.

[12] Rapulenyane N, Antunes E, Masilela N, Nyokong T. Synthesis and photophysicochemical properties of novel zinc phthalocyanines mono substituted with carboxyl containing functional groups. J Photochem Photobiol A Chem 2012;250:18–24.

[13] Makhseed S, Tuhl A, Samuel J, Zimcik P, Al-Awadi N, Novakova V. New highly soluble phenoxy-substituted phthalocyanine and azaphthalocyanine derivatives: synthesis, photochemical and photophysical studies and atypical aggregation behavior. Dyes Pigment 2012;95:351–7.

[14] Saka ET, Gol C, Durmus M, Kantekin H, Biyikhoglu Z. Photophysical, photochemical and aggregation behavior of novel peripherally tetra-substituted phthalocyanine derivatives. J Photochem Photobiol A Chem 2012;241:67–78.

[15] Zhang XF, Guo WF. Imidazole functionalized magnesium phthalocyanine photosensitizer: modified photophysics, singlet oxygen generation and photooxidation mechanism. J Phys Chem A 2012;116:7651–7.

[16] Tombe S, Chidawanyika W, Antunes E, Priniotakis G, Westbroek P, Nyokong T. Physicochemical behavior of zinc tetrakis (benzylmercapto) phthalocyanine when used to functionalize gold nanoparticles and in electronspun fibers. J Photochem Photobiol A Chem 2012;240:50–8.

[17] Uslan C, Sesalan BS. Synthesis of novel DNA-interacting phthalocyanines. Dyes Pigment 2012;94:127–35.

[18] Zeballos NCL, Vior MCG, Awruch J, Dicelio LE. An exhaustive study of a novel sulfur-linked adamantane tetrasubstituted zinc(II) phthalocyanine incorporated into liposomes. J Photochem Photobiol A Chem 2012;235:7–13.

[19] Uslan C, Sesalan BS, Durmus M. Synthesis of new water soluble phthalocyanines and investigation of their photochemical, photophysical and biological properties. J Photochem Photobiol A Chem 2012;235:56–64.

[20] Pereira JB, Carvalho EFA, Faustino MAF, Fernandes R, Neves M, Cavaleiro JAS, et al. Phthalocyanine thio-pyridinium derivatives as antibacterial photosensitizers. Photochem Photobiol 2012;88:537–47.

[21] Nombona N, Antunes E, Chidawanyika W, Kleyi P, Tshentu Z, Nyokong T. Synthesis, photophysics and photochemistry of phthalocyanine-epsilon-polylysine conjugates in the presence of metal nanoparticles against *Staphylococcus aureus*. J Photochem Photobiol A Chem 2012;233:24–33.

[22] Ke MR, Yeung SL, Fong WP, Ng DKP, Lo PC. A phthalocyanine-peptide conjugate with high in vitro photodynamic activity and enhanced in vivo tumor-retention property. Chem Eur J 2012;18:4225–33.

[23] Nombona N, Maduray K, Antunes E, Karsten A, Nyokong T. Synthesis of phthalocyanine conjugates with gold nanoparticles and liposomes for photodynamic therapy. J Photochem Photobiol B Biol 2012;107:35–44.

[24] Ke MR, Ng DKP, Lo PC. A pH-responsive fluorescent probe and photosensitiser based on a self-quenched phthalocyanine dimer. Chem Commun 2012;48:9065–7.

[25] Iqbal Z, Masilela N, Nyokong T, Lyubimtsev A, Hanack M, Ziegler T. Spectral, photophysical and photochemical properties of tetra- and octaglycosylated zinc phthalocyanines. Photochem Photobiol Sci 2012;11:679–86.

[26] Zhang XF, Guo WF. Indole substituted zinc phthalocyanine: improved photosensitizing ability and modified photooxidation mechanism. J Photochem Photobiol A Chem 2011;225:117–24.

[27] Durmus M, Yaman H, Gol C, Ahsen V, Nyokong T. Water-soluble quaternized mercaptopyridine-substituted zinc-phthalocyanines: synthesis, photophysical, photochemical and bovine serum albumin binding properties. Dyes Pigment 2011;91:153–63.

[28] Vior MCG, Monteagudo E, Dicelio LE, Awruch J. A comparative study of a novel lipophilic phthalocyanine incorporated into nanoemulsion formulations: photophysics, size, solubility and thermodynamic stability. Dyes Pigment 2011;91:208–14.

[29] Piskin M, Durmus M, Bulut M. Highly soluble 7-oxy-3-(4-methoxyphenyl) coumarin bearing zinc phthalocyanines: synthesis and investigation of photophysical and photochemical properties. J Photochem Photobiol A Chem 2011;223:37–49.

[30] Gmurek M, Kubat P, Mosinger J, Miller JS. Comparison of two photosensitizers Al(III) phthalocyanine chloride tetrasulfonic acid and meso-tetrakis(4-sulfonatophenyl)porphyrin in the photooxidation of n-butylparaben. J Photochem Photobiol A Chem 2011;223:50–6.

[31] Yuksel F, Durmus M, Ahsen V. Photophysical, photochemical and liquid-crystalline properties of novel gallium(III) phthalocyanines. Dyes Pigment 2011;90:191–200.

[32] Biyiklioglu Z, Durmus M, Kantekin H. Tetra-2-[2-(dimethylamino)ethoxy] ethoxy substituted zinc phthalocyanines and their quaternized analogues: synthesis, characterization, photophysical and photochemical properties. J Photochem Photobiol A Chem 2011;222:87–96.

[33] Zhang XF, Rong YL. Silicon tetrabenzotriaza corrole and silicon phthalocyanine: synthesis, photophysics and singlet oxygen generation. J Photochem Photobiol A Chem 2011;222:141–5.

[34] Camur M, Durmus M, Bulut M. Coumarino-12-crown-4 bearing phthalocyanine photosensitizers for singlet oxygen production. J Photochem Photobiol A Chem 2011;222:266–75.

[35] Chauke VP, Arslanoglu Y, Nyokong T. Synthesis and photophysical behaviour of tantalum and titanium phthalocyanines in the presence of gold nanoparticles: photocatalysis towards the oxidation of cyclohexene. J Photochem Photobiol A Chem 2011;221:38–46.

[36] Lau JTF, Lo PC, Fong WP, Ng DKP. Preparation and photodynamic activities of silicon(IV) phthalocyanines substituted with permethylated beta-cyclodextrins. Chem Eur J 2011;17:7569–77.

[37] Camur M, Ahsen V, Durmus M. The first comparison of photophysical and photochemical properties of non-ionic, ionic and zwitterionic gallium (III) and indium (III) phthalocyanines. J Photochem Photobiol A Chem 2011;219: 217–27.

[38] Mantareva V, Kussovski V, Angelov I, Wohrle D, Dimitrov R, Popova E, et al. Non-aggregated Ga(III)-phthalocyanines in the photodynamic inactivation of planktonic and biofilm cultures of pathogenic microorganisms. Photochem Photobiol Sci 2011;10:91–102.

[39] Garcia AM, Alarcon E, Munoz M, Scaiano JC, Edwards AM, Lissi E. Photophysical behaviour and photodynamic activity of zinc phthalocyanines associated to liposomes. Photochem Photobiol Sci 2011;10:507–14.

[40] Stuchinskaya T, Moreno M, Cook MJ, Edwards DR, Russell DA. Targeted photodynamic therapy of breast cancer cells using antibody-phthalocyanine-gold nanoparticle conjugates. Photochem Photobiol Sci 2011;10:822–31.

[41] Liu ZJ, Xiong XQ, Li Y, Li SY, Qin JG. Synthesis, optical properties and singlet oxygen generation of a phthalocyanine derivative containing strong two-photon-absorbing chromophores in the periphery. Photochem Photobiol Sci 2011;10:1804–9.

[42] Hahn U, Setaro F, Ragas X, Gray-Weale A, Nonell S, Torres T. Microenvironment-switchable singlet oxygen generation by axially-coordinated hydrophilic ruthenium phthalocyanine dendrimers. Phys Chem Chem Phys 2011;13:3385–93.

[43] Tuhl A, Makhseed S, Zimcik P, Al-Awadi N, Novakova V, Samuel J. Heavy metal effects on physicochemical properties of non-aggregated azaphthalocyanine derivatives. J Porphyrins Phthalocyanines 2012;16:817–25.

[44] Donzello MP, Viola E, Giustini M, Ercolani C, Monacelli F. Tetrakis(thiadiazole) porphyrazines. 8. Singlet oxygen production, fluorescence response and liposomal incorporation of tetrakis(thiadiazole)porphyrazine macrocycles [TTDPzM] (M = MgII(H2O), ZnII, AlIIICl, GaIIICl, CdII, CuII, 2HI). Dalton Trans 2012;41:6112–21.

[45] Solov'ev KN, Borisevich EA. Intramolecular heavy-atom effect in the photophysics of organic molecules. Phys Usp 2012;48:231–53.

[46] Maree S, Phillips D, Nyokong T. Synthesis, photophysical and photochemical studies of germanium and tin phthalocyanine complexes. J Porphyrins Phthalocyanines 2002;6:17–25.

[47] Seotsanyana-Mokhosi I, Maree S, Maree MD, Nyokong T. Photochemical studies of binuclear phenoxysubstituted phthalocyanines containing catecholate bridges. J Porphyrins Phthalocyanines 2003;7:167–75.

[48] Carmichael I, Hug GL. Triplet–triplet absorption spectra of organic molecules in condensed phases. J Phys Chem Ref Data 1986;15. 1–250.

[49] Lagorio MG, Dicelio LE, Roman EAS, Braslavsky SE. Quantum yield of singlet molecular oxygen sensitization by copper(II) tetracarboxyphthalocy anine. J Photochem Photobiol B Biol 1989;3:615–24.

[50] Kuznetsova N, Gretsova N, Kalmykova E, Makarova E, Dashkevich S, Negrimovskii V, et al. 31 Study of spectral properties of zinc phthalocyanines used as sensitizers in photodynamic therapy. Russ J Gen Chem 2000;70:133–9.

[51] Ma C, Tian D, Hou X, Chang Y, Cong F, Yu H, et al. Synthesis and characterization of several soluble tetraphenoxy-substituted copper and zinc phthalocyanines. Synthesis 2005;2005:741–8.

[52] Durmuş M, Nyokong T. Synthesis, photophysical and photochemical properties of aryloxy tetra-substituted gallium and indium phthalocyanine derivatives. Tetrahedron 2007;63:1385–94.

[53] Cong F, Li J, Ma C, Gao J, Duan W, Du X. Tuning J-type dimers of non-peripherally substituted zinc tetra-4-tert-butylphenophthalocyanine. Spectrochim Acta A Mol Biomol Spectrosc 2008;71:1397–401.

[54] Tau P, Nyokong T. Synthesis and electrochemical characterisation of α- and β-tetra-substituted oxo(phthalocyaninato) titanium(IV) complexes. Polyhedron 2006;25:1802–10.

[55] Papageorgiou N, Ferro Y, Salomon E, Allouche A, Layet JM. Geometry and electronic structure of lead phthalocyanine: quantum calculations via density-functional theory and photoemission measurements. Phys Rev B 2003;67: 235105.

[56] Iyechika Y, Yakushi K, Ikemoto I, Kuroda H. Structure of lead phthalocyanine (triclinic form). Acta Crystallogr B 1982;38:766–70.

[57] Ukei K. Lead phthalocyanine. Acta Crystallogr B 1973;29:2290–2.

[58] Atkins PW, Friedman RS. Molecular quantum mechanics. New York, NY: Oxford University Press; 1997.

[59] Zhang XF, Wang Y, Niu L. Titanyl phthalocyanine and its soluble derivatives: highly efficient photosensitizers for singlet oxygen production. J Photochem Photobiol A Chem 2010;209:232–7.

[60] Zhang XF, Xi Q, Zhao J. Fluorescent and triplet state photoactive J-type phthalocyanine nano assemblies: controlled formation and photosensitizing properties. J Mater Chem 2010;20:6726–33.

[61] Zhang X-F, Huang J, Xi Q, Wang Y. The excited triplet state properties of titanyl phthalocyanine and its sulfonated derivatives. Aust J Chem 2010;63:1–6.

[62] Redmond WR, Gamlin JN. 21 A compilation of singlet oxygen yields from biologically relevant molecules. Photochem Photobiol 1999;70:391–475.